NANO LETTERS

2001
Vol. 1, No. 6
309−314

Light Trapped in a Photonic Dot: Microspheres Act as a Cavity for Quantum Dot Emission

Mikhail V. Artemyev,[†] Ulrike Woggon,*[,†] Reinhold Wannemacher,[‡] Heiko Jaschinski,[†] and Wolfgang Langbein[†]

Department of Physics, University of Dortmund, Otto-Hahn-Strasse 4, D-44221 Dortmund, Germany, and Institute of Physics, University of Technology Chemnitz, Reichenhainer Strasse 70, D-09107 Chemnitz, Germany

Received April 29, 2001

ABSTRACT

Optical microcavities that confine the propagation of light in all three dimensions (3D) are fascinating research objects to study 3D-confined photon states, low-threshold microlasers, or cavity quantum electrodynamics of quantum dots in 3D microcavities. A challenge is the combination of complete electronic confinement with photon confinement, e.g., by linking a single quantum dot to a single photonic dot. Here we report on the interplay of 3D-confined cavity modes of single microspheres (the photonic dot states) with photons emitted from quantized electronic levels of single semiconductor nanocrystals (the quantum dot states). We show how cavity modes of high cavity finesse are switched by single, blinking quantum dots. A concept for a quantum-dot microlaser operating at room temperature in the visible spectral range is demonstrated. We observe an enhancement in the spontaneous emission rate; i.e., the Purcell effect is found for quantum dots inside a photonic dot.

Spherical microcavities of a few micrometers in diameter show sharp, spectrally well-separated cavity modes in the visible spectral range. These eigenmodes of a 3D microcavity are characterized by the angular quantum number l and radial quantum number n for the transverse electric (TE_l^n) and transverse magnetic (TM_l^n) field modes. The optical quality of a microcavity is defined by $Q = \omega_{cav}/\Delta\omega_{cav}$, the ratio between resonance frequency ω_{cav} and bandwidth $\Delta\omega_{cav}$ of a cavity mode. High Q values mean narrow modes and efficient light trapping inside the microcavity. When a light-emitting dipole, for example, a semiconductor nanocrystal (quantum dot (QD)), is inserted into a 3D microcavity and its eigenfrequency ω_{QD} is resonant with a high-Q cavity mode ω_{cav}, then the confined photonic and electronic states interact and a new coupled quantum-mechanical system evolves with a coupling strength defined by the Rabi splitting Ω_R (see, e.g., refs 1−6). Semiconductor quantum dots inside a 3D microcavity (photonic dot (PD)), a structure we will designate from now on as QDs@PD, provide a fascinating artificial system to study light−matter interaction in confined systems. The examples presented here apply to the regime of weak coupling, i.e., $\Omega_R < \Delta\omega_{cav}$.

Figure 1 shows a representative QDs@PD structure based on a glass microsphere. The emission characteristics of a luminescent CdSe nanocrystal will completely change when it is incorporated into a 3D microcavity, as illustrated by the theoretical emission pattern plotted in Figure 1. As can be seen in the single mode pattern of a so-called whispering gallery mode, the electromagnetic field is highest close to the surface of the sphere. Therefore, to study the combined 3D confinement of electrons and photons, most promising are concepts with QDs attached to the surface of a bulk microsphere or embedded in the thin shell of hollow microspheres doped with QDs.[7−9] We choose as light-emitting dipoles highly luminescent ZnS-coated CdSe nanocrystals[10] (diameter ∼4.5 nm). These nanocrystals are chemically bonded to the surface of glass microspheres (diameter 3−10 μm) via mercaptosilanes.[11] The mercapto groups form a monolayer shell on the glass surface and are used to bind CdSe nanocrystals. In this process, parts of the stabilizing TOPO/TOP molecules are replaced by sulfur, which compensates dangling bonds formed by Zn atoms. The deposited shell of mercapto groups and nanocrystals is of subwavelength thickness and within the range of the evanescent electromagnetic field formed at the sphere−shell interfaces. Either a large amount of or only a few QDs can be attached to a single microsphere by controlling the concentration of CdSe QDs and the chemical reaction time.[12]

* Corresponding author. E-mail: woggon@fred.physik.uni-dortmund.de. Phone: ++49-(0)231 755 3767. Fax: ++49-(0) 231 755 3674).
[†] University of Dortmund.
[‡] University of Technology Chemnitz.

10.1021/nl015545l CCC: $20.00
Published on Web 05/25/2001

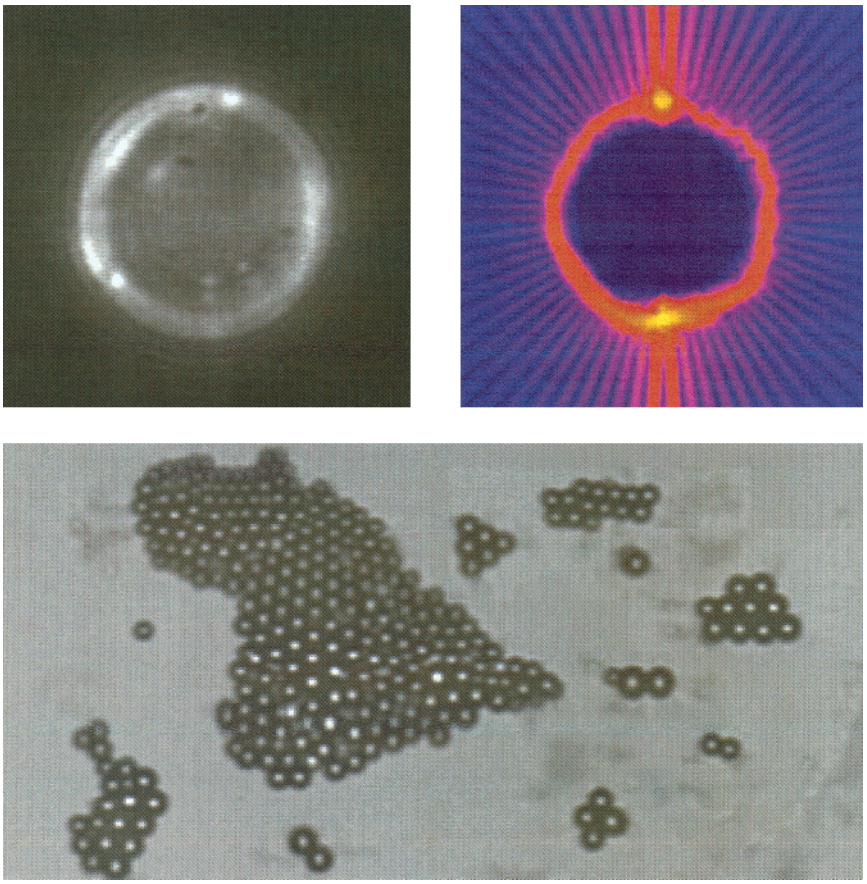

Figure 1. Upper left: microscope image of a glass microsphere doped with a small number of CdSe nanocrystals in a thin surface shell (radius $R = 4.1\ \mu$m). Upper right: Calculated electromagnetic field distribution inside and outside a spherical microcavity containing a single emitting nanocrystal placed close to the surface of a sphere ($R = 2.8\ \mu$m, refraction index $n = 1.5$) and being in resonance with the cavity mode TM_{36}^{1}. Plotted is the time-averaged Pointing vector on a logarithmic scale ranging from 10^0 to 10^5 arbitrary units. Lower panel: an arrangement of spheres showing single photonic dots, photonic dot "molecules", lines, and ordered arrays of microspheres doped with CdSe nanocrystals.

To analyze the optical properties of our QDs@PD-structures, the photoluminescence spectra (PL) are measured as shown for representative PDs in Figure 2. For CdSe QDs without a cavity, Figure 2 shows additionally the inhomogeneously broadened absorption (αd-spectrum in the inset) and emission spectrum (PL). The blue shift of the QD-absorption band by ~100 nm with respect to bulk CdSe indicates the strong electronic quantum confinement effect.[13] If the QDs are now attached to a PD, the emission spectrum of the QD ensemble drastically changes into a discrete number of sharp peaks, the so-called whispering gallery modes (WGMs) of the PD. The small size of the PD ensures a large mode spacing. For $R_{PD} = 2.8\ \mu$m, the cavity modes are separated in energy by a few tens of millielectronvolts, comparable to or even larger than the emission line width $\hbar\Delta\omega_{QD}$ of a single CdSe QD. The room-temperature homogeneous line width $\hbar\Delta\omega_{QD}$ for single CdSe QDs has been determined as 50−70 meV (see Figure 2a) decreasing to $\hbar\Delta\omega_{QD} \sim 0.2-1$ meV at $T = 20$ K. For the cavity mode widths $\hbar\Delta\omega_{cav,}$ values between 250 μeV and 1.5 meV were observed, as shown for a representative photonic dot with $R_{PD} = 3.1\ \mu$m in Figure 2b. For a few PDs the observed line widths yield even Q factors $\geq 10^4$, limited by the instrumental resolution. In Figure 2b we assign quantum numbers to the experimental cavity modes using standard Mie theory. The eigenmodes calculated for the ideal spherical microcavity indicate the only energy states (confined photonic states) into which the quantum dot emission is allowed. For PD parameters of $R_{theo} = 3.041\ \mu$m and refraction index $n = 1.485$, good agreement with the experiment is achieved (dispersion of the glass and possible asphericity of the PD have been neglected in the calculation).

To demonstrate the possibility to couple only a single QD to a single mode of a PD, we exploit the well-established effect of photoluminescence-blinking from single nanocrystals.[14,15] It is illustrated in Figure 3a. The current model to explain blinking of QDs, i.e., the observed temporal fluctuations in radiative recombination probability, is based on the idea that the charge state of a quantum dot may change due to carrier escape.[14] The simultaneous changes in the surrounding local electric fields result in correlations between intensity fluctuations and spectral diffusion. Spectral jumps of the emission peaks of up to a few tens of millelectronvolts at $T = 10$ K have been observed for single QD emission.[15] Figure 3a illustrates the blinking effect at room temperature for a single QD on glass.[16] Here, the magnitude of the spectral jumps is comparable with the mode spacing of the PD. In a single QD@PD structure containing only a single

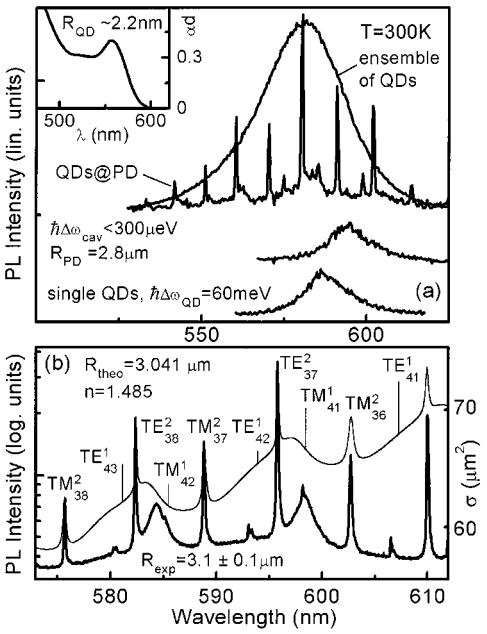

Figure 2. (a) Room-temperature emission spectra of quantum dots before and after attaching them to a single photonic dot. Plotted are the spectra for an ensemble of QDs, single QDs, and an ensemble of QDs incorporated in a thin surface shell of a PD. Inset: Absorption spectrum of the QD ensemble. The QD emission is excited nonresonantly by a focused Ar-ion laser ($\lambda = 488$ nm, $I_{pump} = 50$ W/cm^2) and detected by use of a microscope objective with a numerical aperture of 0.95, an imaging spectrometer and a CCD camera ($\sim$0.4 μm spatial resolution, $\sim$0.08 nm spectral resolution) for a single PD selected by a pinhole. (b) Emission spectrum of a $R_{PD} = 3.1$ μm PD taken with a factor of 4 higher spectral resolution for the spectral range around 595 nm (thick line). For the experimental cavity, Q values of $\sim$7500 have been determined. For comparison, the calculated scattering cross section σ characterizing the cavity eigenmodes is shown (thin line). The most pronounced PD eigenstates are labeled by their quantum numbers TE/TM, l and n. Within the detected spectral window the quantum numbers vary between $l = 32$ and $l = 42$ with $n = 1, 2$ for the sharp modes while modes with $n \geq 3$ form the weak background.

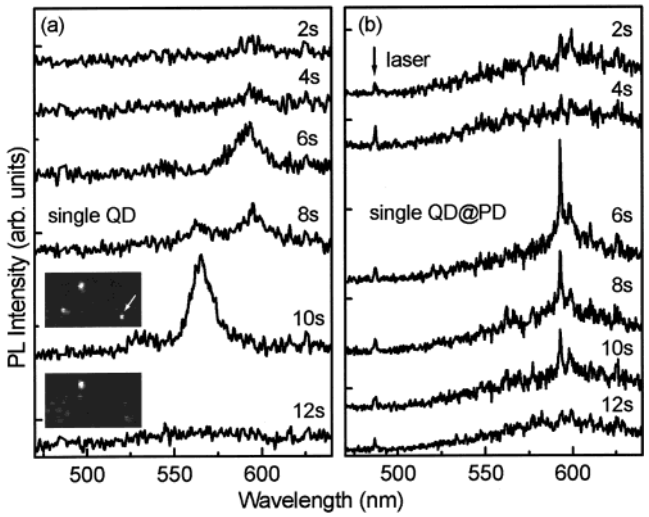

Figure 3. (a) Room-temperature emission spectrum of a single CdSe QD (without cavity) taken at different observation times to illustrate the blinking effect in nanocrystals. (b) Same experiment for a single QD but now bound to a PD. The emission of the quantum dot switches two very sharp modes of high Q (mode width below spectral resolution). The signal from scattered laser light is shown too, to exclude any correlation with fluctuations in pump intensity.

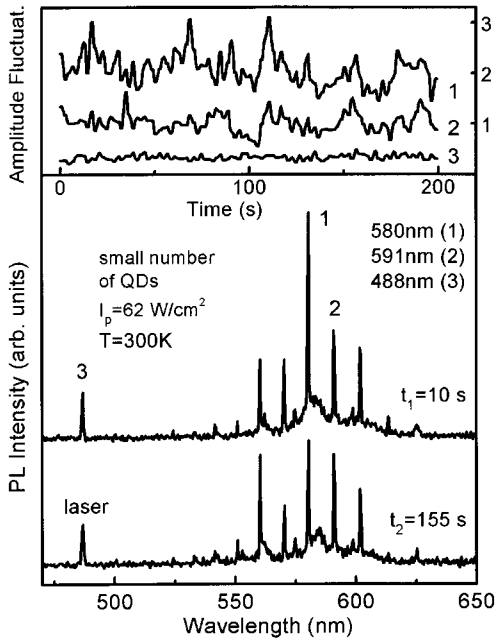

Figure 4. Intensity fluctuations of different cavity modes when several QDs are bound to the surface of a glass microsphere. The inset shows the statistics in emission within a time window of 200 s. Blinking in-phase over a time of $\sim$120 s is observed.

CdSe QD, the QD should switch single modes of the PD "on" and "off" according to its blinking frequency. Indeed, as demonstrated in Figure 3b, a single QD can switch in time the modes of a PD! Also, a sequential coupling of QD emission to neighboring PD modes should be possible when the effect of spectral diffusion could be controlled. In the process of spectral diffusion, the cavity might act as a spectral filter, which allows only the observation of nanocrystals without spectral jumps or with spectral shifts equal to the cavity mode distance. If no cavity modes exist in the spectral window of spectral diffusion, after a spectral jump the nanocrystals become optically inactive.

Figure 4 illustrates the emission characteristics of a QDs@PD system when the number of QDs is gradually increased. Several emission bands from individual QDs are now weakly overlapping, both temporally and spectrally, and we observe a statistical mode blinking on a millisecond to second time scale at room temperature. About two modes can be excited by the same single QD. The insert of Figure 4 shows that these modes can blink in phase as long as the switching quantum dot does not undergo a spectral jump (here about 2 min). Out-of-phase blinking occurs if a spectrally neigboring QD is the object of spectral diffusion, shifting its emission into the considered spectral range but covering only one of the two peaks. Then dots with different blinking frequencies are superposited and the blinking modes are no more in phase. With an increasing number of QDs per PD, averaging over many QD emission bands results in a decrease in the amplitude fluctuations of cavity modes. In

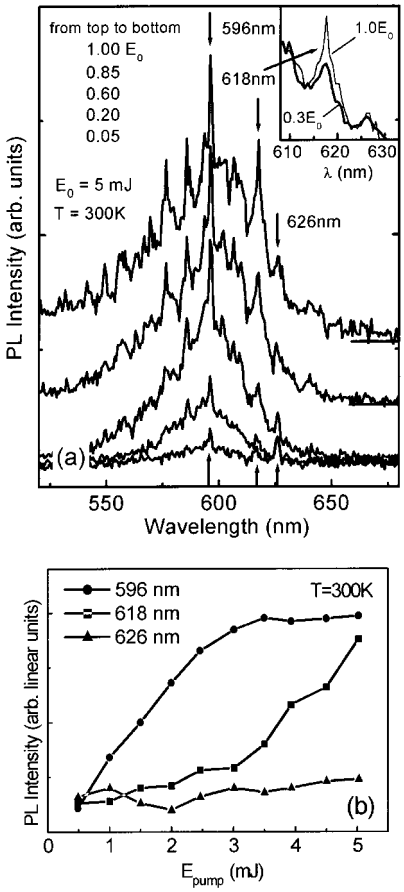

Figure 5. Analysis of $I_{PL} = f(I_{pump})$ for a low-Q QDs@PD-structure with a large amount of QDs under pulsed excitation by 3 ns pulses of an optical-parametric oscillator (490 nm) pumped by a Nd:YAG laser (30 Hz repetition rate), focused to a spot of $d = 500\ \mu$m. For the cavity mode at 618 nm threshold characteristics and mode narrowing are shown, indicating the onset of lasing. Mode competition between the 626 and 618 nm modes is observed. In all spheres studied, no threshold is found for the central modes, e.g., like the mode at 596 nm.

a dense ensemble of QDs the blinking effect eventually disappears.

A QD@PD structure is a very promising object to design an optically pumped QD-based microlaser emitting in the visible spectral range at room temperature. Optical gain has been already detected for CdSe QDs at low and room temperatures.[17−19] Since a detailed theory of lasing processes in 3D microcavities is presently not available yet, we start from an experimental approach and report our observations with respect to the change in the mode-emission intensity I_{PL} when the pump intensity I_{pump} is increased. In the present literature about lasing in microspheres (see, e.g., refs 20−24), two features are quoted to evidence lasing: (i) a threshold behavior in the $I_{PL} = f(I_{pump})$ characteristics and (ii) mode narrowing in the spectral response. Both features can be observed in a QD@PD structure with low Q factor (∼2000). For the experiment we excite the nanocrystals with 3 ns pulses of an optical-parametric oscillator (490 nm) pumped by a Nd:YAG laser (30 Hz repetition rate). The maximum pump energy is $E_0 = 5$ mJ. Parts a and b of Figure 5 give an overview about typical $I_{PL} = f(I_{pump})$ characteristics observed at room temperature in the visible spectral range. Three typical behaviors are found for the mode intensity and summarized in Figure 5b: For the central modes (e.g., for the 596 nm mode) no threshold and only a steep increase followed by saturation at the highest pump power are found. For modes in the tail of the inhomogeneously broadened PL band a pronounced threshold is observed even for low-Q modes (e.g., for the 618 nm mode). Also, in the low-energy tail, mode competition is found, which prevents the onset of lasing (e.g., for the 626 nm mode). Since in a pulsed experiment comparatively high pump power can be applied without thermal effects, these low-Q cavity modes can be also used to demonstrate the effect of line narrowing, as can be seen for the 618 nm mode above a threshold of ∼1 mJ (right insert). Summarizing Figure 5a,b, one can see that for low-Q cavities, threshold behavior and spectral narrowing become evident when the pump power is increased. However, both the Q factor and the spectral positions of the cavity modes within the inhomogeneously broadened QD-emission band have distinct influence on the $I_{PL} = f(I_{pump})$ characteristics. For high-Q cavities we observe rather a behavior similar to that of the central modes. A plot of the $I_{PL} = f(I_{pump})$ characteristics in a double-log plot results in slopes close to ∼1, which is a hint that biexcitonic processes are not dominating in the emission process for the used range of pump intensities, both in pulsed and continuous wave (cw) experiments. The study of lasing in high-Q cavities requires more detailed experimental and theoretical work in the future.

Finally, we present low-temperature experiments at QDs@PD structures and study the dynamics of radiative emission of 3D-confined electronic states in a 3D microcavity. A fundamental principle of cavity-quantum electrodynamics is the modification of the spontaneous emission rate inside a high-Q microcavity, which was theoretically predicted by Purcell[25] in 1946. An enhancement of the spontaneous emission rate is expected if the lifetime of photons in the cavity is shorter than the radiative lifetime of the light-emitting species, i.e., for our QDs@PD structures $\Delta\omega_{QD} \leq \Delta\omega_{cav}$ has to be fulfilled, which holds in a temperature range $T \leq 20$ K. The modification of the spontaneous emission rate is given by the Purcell factor $F = \tau_{free}/\tau_{cav} = 3Q(\lambda_c/n)^3/(4\pi^2 V_{eff})$ (see ref 2), which shows that further important parameters are the mode volume V_{eff} and the cavity quality factor Q (λ_c is the wavelength of cavity photons and n the effective refractive index). The inset of Figure 6 shows the spectral widths for single QDs and PD modes of average (representative) quality ($\Delta\omega_{QD} \sim 0.3$ meV, $\Delta\omega_{cav} = 0.285$ meV, $Q = 7434$). Since the spectral line width of the single QDs has additional contributions from pure dephasing, the radiative decay time of the uncoupled nanocrystals is longer than the cavity decay time; i.e., we fulfill the condition $\tau_{QD} \geq \tau_{cav}$. For the experiments two samples have been prepared: one is a high-Q glass microsphere; the other, a small piece of glass as reference, e.g., from a broken microsphere. Both are impregnated with CdSe QDs in the same process, thus eliminating all variations arising from chemical preparation. The samples are absolutely identically despite the presence or absence of the

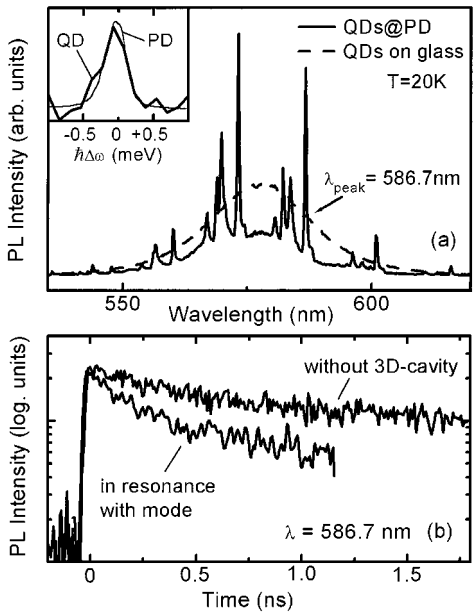

Figure 6. (a) Low-temperature emission spectra of a high-Q QDs@PD-structure and a reference ensemble of CdSe QDs on glass prepared under identical experimental conditions. Inset: Spectral line widths at $T = 20$ K measured in a separate experiment with highest spectral resolution for a representative single CdSe QD and a representative PD mode. (b) Dynamics of radiative emission measured at $T = 20$ K at 586.7 nm after excitation by a 120 fs pulse at 445 nm (frequency-doubled Ti:Sa laser). The emission is detected spatially and spectrally and is temporally resolved using a microscope objective (spatial resolution 0.5 μm), an imaging spectrometer (spectral resolution 0.1 nm), and a Streak camera (time resolution 20 ps). For the CdSe QDs on glass a monoexponential decay is found with a radiative lifetime of 1.1 ns, for QDs on PD a decrease in decay time is observed, resulting in fast initial decay with 220 ps.

spherical cavity. To avoid the influence of nonradiative recombination caused by trap processes, we optimized before the preparation route and used only those nanocrystal preparation techniques that result in QDs of high quantum efficiency (~50%, see ref 16) and monoexponential decay curves with lifetimes in the range of a few nanoseconds. The chemical link to the glass surface results in a different surface configuration as usual for colloidal nanocrystals. We suppose that the QD dynamics here is more similar to the behavior known for CdSe nanocrystals embedded in glass exhibiting lifetimes in the nanosecond range.[26] In the following experiment we excite the QD emission with 120 fs pulses and compare the decay time for QDs with and without a 3D cavity. In this experiment we do not fulfill the condition to observe gain confirmed by the measured $I_{PL} = f(I_{pump})$ dependence under low-power femtosecond excitation. In Figure 6 we compare the dynamics of QD emission for an ultranarrow cavity mode and QDs emitting into free space. We analyze the decay times spectrally resolved and concentrate on the low-energy part of the emission spectrum. In this spectral range we can neglect the influence of relaxation dynamics, in particular between bright and dark states, since we select the largest QDs for which the exchange splitting effect is small (at ~2 eV, were the experiments are performed, the exchange splitting we measured is about 1 meV[27] and at 20 K we have a sufficient thermal population of the allowed transition). Likewise, the excitation density is so low that Augerrecombination can be excluded (as confirmed by the monoexponential decay observed for the CdSe QDs without cavity). Analyzing the results shown in Figure 6 we clearly see a fastening of the intial decay time. Since the only difference between the two samples is the additional cavity, we assign the observed modification of radiative decay to a cavity effect. For the different cavity modes and PD sizes studied, the decay times in the cavity are enhanced by a factor between 3 and 5, varying for the different modes because of variations in Q and mode volume. The comparison of the decay times on- and off-resonant to a cavity mode results likewise in a decrease in decay time. The enhancement factor, however, is smaller, around 2, which we explain by the contribution of weaker modes of higher l and n having a larger mode volume and forming the background of the cavity spectrum, as derived from the calculations related to Figure 2. One of the most pronounced modifications is shown for a selected cavity mode at 586.7 nm with an enhancement in the spontaneous emission rate by a factor ~5 in QDs@PD as compared to QDs on glass. We assume that here predominantly high-Q modes propagating within a small ring close to the surface with very small mode volume contribute to this strong change in the decay rate (comparable to 2D microdisks but with less leakage modes). Calculations of the electromagnetic field distribution have shown that high-Q whispering gallery modes can become concentrated in such rings or thin shells.[15] Estimating the Purcell factor F for such a ring with a cross sectional area of the order of $(\lambda_c/n)^2$, and radius $r \sim R_{PD}$, we obtain values for F between 2 and 10, depending on the quality factor Q. This is of the same order of magnitude as the experimentally observed values.

The study of QDs@PD structures, demonstrated here in a few initial experiments, reveals many fascinating questions and fundamental problems that appear when merging two main concepts of solid-state physics, the complete 3D electronic and photonic confinement, in one structure.

Acknowledgment. We thank T. Lottermoser and D. Fröhlich for providing the nanosecond laser system and experimental support in the high-density gain measurements. Financial support by the Volkswagen Foundation and the Deutsche Forschungsgemeinschaft is grateful acknowledged.

References

(1) Chang, R. K., Chamillo, A. J., Eds. *Optical Processes in Microcavities*; Advanced Series in Applied Physics Vol. 3; World Scientific: Singapore, 1996.
(2) Benisty, H., Gerard, J. M., Houdre, R., Rarity, J., Weisbuch, C., Eds. *Confined Photon Systems*; Lecture Notes in Physics 531; Springer-Verlag: Berlin, 1999.
(3) Yamamoto, Y.; Tassone, F.; Cao, H. *Semiconductor Cavity Quantum Electrodynamics*; Springer Tracts in Modern Physics 169; Springer-Verlag: Berlin, 2000.
(4) Agarwal, G. S. *J. Modern Opt.* **1998**, *45*, 449.
(5) Vernooy, D. W.; Furusawa, A.; Georgiades, N. P.; Ilchenko, V. S.; Kimble, H. J. *Phys. Rev. A* **1998**, *57*, R2293.
(6) Gerard, J. M.; Sermage, B.; Gayral, B.; Legrand, B.; Costard, E.; Thierry-Meig, V. *Phys. Rev. Lett.* **1998**, *81*, 1110.

(7) Xudong, F.; Palingidis, P.; Lacey, S.; Wang, H.; Lonergan, M. *Opt. Lett*. **2000**, *25*, 1600.
(8) Artemyev, M.; Woggon, U. *Appl. Phys. Lett.* **2000**, *76*, 1353.
(9) Artemyev, M.; Woggon, U.; Wannemacher, R. *Appl. Phys. Lett.* **2001**, *78*, 1032.
(10) Hines, M. A.; Guyot-Sionnest, P. *J. Phys. Chem*. **1996**, *100*, 468.
(11) Goss, C. A.; Charych, D. H.; Majda, M. *Anal. Chem*. **1991**, *63*, 85.
(12) Briefly, the preparation method comprises the following processes: 5 mg of glass spheres (Polyscience Inc.) are treated for 10 min in 3% solution of (3-mercaptopropyl)trimethoxysilane (MPTS) in toluene at 80 °C under vigorous stirring followed by a 4-fold washing in fresh toluene. This procedure results in a near monolayer of MPTS on the surface of the glass spheres. Then the spheres with the MPTS-activated surface are mixed with a highly diluted colloidal solution of (CdSe)ZnS quantum dots in toluene. Under stirring, the (CdSe)-ZnS dots are bound to the surface of glass spheres via formation of S−Zn chemical bonds between surface Zn atoms and MPTS mercapto groups.
(13) Woggon, U. *Optical Properties of Semiconductor Quantum Dots*; Springer Tracts in Modern Physics 136; Springer-Verlag: Berlin, Heidelberg, 1997.
(14) Empedocles, S. A.; Neuhauser, R.; Shimizu, K.; Bawendi, M. G. *Adv. Mater*. **1999**, *11*, 1243.
(15) Neuhauser, R.; Shimizu, K. T.; Woo, W. K.; Empedocles, S. A.; Bawendi, M. G. *Phys. Rev. Lett*. **2000**, *85*, 3301.
(16) The blinking of quantum dots observed here has nothing in common with the analysis of the photon statistics to study nonclassical light sources. However, because the blinking effects are observed on time scales of seconds, it should not exclude performing experiments of cavity-QED on picosecond time scales, such as the search for Rabi oscillations in QD@PD structures.
(17) Gindele, F.; Westphäling, R.; Woggon, U.; Spanhel, L.; Ptatschek, V. *Appl. Phys. Lett.* **1997**, *71*, 2181.
(18) Giessen, H.; Woggon, U.; Fluegel, B.; Mohs, G.; Hu, Y. Z.; Koch, S. W.; Peyghambarian, N. *Chem. Phys.* **1996**, *210*, 71.
(19) Klimov, V. I.; Mikhailovsky, A. A.; Su, X.; Malko, A.; Hollingsworth, J. A.; Leatherdale, C. A.; Eisler, H. G.; Bawendi, M. G. *Science* **2000**, *290*, 314.
(20) Pelton, M.; Yamamoto, Y. *Phys. Rev. A* **1999**, *59*, 2418.
(21) Nagai, M.; Hoshino, F.; Yamamoto, S.; Shimano, R.; Kuwata-Gonokami, M. *Opt. Lett.* **1997**, *22*, 1630.
(22) Treussart, F.; Ilchenko, V. S.; Roch, J. F.; Domokos, P.; Hare, J.; Lefevre, V.; Raimond, J.-M.; Haroche, S. *J. Luminescence* **1998**, *76*−*77*, 670.
(23) Fujiwara, H.; Sasaki, K. *J. Appl. Phys.* **1999**, *86*, 2385.
(24) Von Klitzing, W.; Jahier, E.; Long, R.; Lissillour, F.; Lefevre-Seguin, V.; Hare, J.; Raimond, J.-M.; Haroche, S. *Electron. Lett.* **1999**, *35*, 1745.
(25) Purcell, E. M. *Phys. Rev*. **1946**, *69*, 681.
(26) Woggon, U.; Wind, O.; Gindele, F.; Tsitsishvili, E.; Müller, M. *J. Lumin.* **1996**, *70*, 269. Woggon, U.; Giessen, H.; Gindele, F.; Wind, O.; Fluegel, B.; Peyghambarian, N. *Phys. Rev. B* **1996**, *54*, 17681.
(27) Woggon, U.; Gindele, F.; Wind, O.; Klingshirn, C. *Phys. Rev. B* **1996**, *54*, 1506.

NL015545L